Phase behavior of a suspension of colloidal hard rods and nonadsorbing polymer

S. V. Savenko[a] and Marjolein Dijkstra
Soft Condensed Matter, Utrecht University, Princetonplein 5, 3584 CC Utrecht, The Netherlands

(Received 28 February 2006; accepted 12 April 2006; published online 15 June 2006)

We study the phase behavior of a mixture of colloidal hard rods with a length-to-diameter ratio of $L/\sigma_c=5$ and nonadsorbing ideal polymer. We map our binary mixture onto an effective one-component system by integrating out the degrees of freedom of the polymer coils. We derive a formal expression for the exact effective Hamiltonian of the colloidal rods, i.e., it includes all effective many-body interactions and it is related to the exact free volume available for the polymer. We determine numerically on a grid the free volume available for the ideal polymer coils "on the fly" for each colloidal rod configuration during our Monte Carlo simulations. This allows us to go beyond first-order perturbation theory, which employs the pure hard-rod system as reference state. We perform free energy calculations for the isotropic, nematic, smectic, and crystal phase using thermodynamic integration and common tangent constructions are used at fixed polymer fugacities to map out the phase diagram. The phase behavior is determined for size ratios $q=\sigma_p/\sigma_c=0.15$, 0.5, and 1, where σ_p is the diameter of the polymer coils. The phase diagrams based on the full effective Hamiltonian are compared with those obtained from first-order perturbation theory, from simulations using the effective pair potential approximation to the effective Hamiltonian, and with those based on an empiric effective depletion potential for the rods. We find that the many-body character of the effective interactions stabilizes the nematic and smectic phases for large q, while the effective pair potential description overestimates the attractive interactions and favors, hence, a broad isotropic-crystal coexistence. © *2006 American Institute of Physics*.
[DOI: 10.1063/1.2202853]

I. INTRODUCTION

The addition of nonadsorbing polymer to a suspension of colloidal rods can be used to purify the rods[1] or to modify the effective interactions between the rodlike particles.[2] The presence of polymer leads to an effective attraction between the rods due to the so-called depletion effect.[3] The range of this attraction is equal to the radius of gyration of the polymer coils and the strength of the attraction is proportional to the fugacity of the polymers.[3,4]

For spherical colloids, a particularly simple model for colloid-polymer mixtures was proposed by Vrij,[4] which is often referred to as the Asakura-Oosawa-Vrij (AO) model. In this model, the colloids are modeled as hard spheres with diameter σ_c, while the polymer coils with diameter σ_p are assumed to be ideal and noninteracting. Moreover, the polymer coils are excluded by a center-of-mass distance of $(\sigma_c+\sigma_p)/2$ from the colloids. In this simple model colloid-polymer mixture, Vrij showed the existence of a spinodal instability. Moreover, the effective two-body or Asakura-Oosawa depletion potential can be calculated analytically for this highly idealized model. Gast *et al.* calculated phase diagrams using this effective pair potential in first-order thermodynamic perturbation theory and employing the hard-sphere system as a reference state.[5] They found that the addition of polymer can give broad fluid-solid coexistence regions, but also stable fluid-fluid and colloidal gas-liquid-solid coexistence, for sufficiently large polymer coils. Similar phase diagrams were determined by Lekkerkerker *et al.* using the so-called free-volume approach[6] and by Meijer and Frenkel using computer simulations with lattice polymers.[7,8] Recently, another approach was followed in Refs. 9–13, which is based on a mapping of the binary mixture onto an effective one-component system. A formal expression for the effective colloid Hamiltonian can be derived by integrating out formally the degrees of freedom of the polymer coils in the partition function.[12–14] This effective Hamiltonian consists of zero-body, one-body, two-body, and higher-body terms, where the two-body (pairwise-additive) term is precisely that given by the Asakura-Oosawa depletion potential. For size ratios $q<2/\sqrt{3}-1\simeq 0.1547$, three- and higher-body terms are zero and the mapping onto an effective Hamiltonian truncated at the effective pair potential level is exact. Full phase diagrams using the two-body (Asakura-Oosawa pair potential) approximation to this effective Hamiltonian were determined by computer simulations.[15] For higher size ratios, however, three- and higher-body effective interactions are not necessarily small. We therefore developed an efficient Monte Carlo simulation scheme for the AO model, based on the exact or full effective colloid Hamiltonian, i.e., it includes all the effective many-body interactions.[12,13] Employing this scheme, we are able to study the full phase diagram and we found that the effective many-body interactions can significantly alter the phase behavior of colloid-polymer

[a]Electronic mail: s.v.savenko@phys.uu.nl

mixtures. In conclusion, the AO model is well studied and well understood by now for colloidal hard spheres. This should be contrasted to the case of nonspherical particles.

The effect of nonadsorbing polymer on the isotropic-nematic transition of rodlike colloids was investigated by Lekkerkerker *et al.*[6] using the perturbation theory. The free volume accessible to the polymers was calculated using the scaled particle theory. Simulations of mixtures of colloidal hard rods with polymer are, however, less advanced. Approximate phase diagrams are determined for hard spherocylinders and ideal polymer using thermodynamic perturbation theory and measuring the free volume available for the polymer in a pure hard-spherocylinder system in simulations.[16] The isotropic-isotropic coexistence was, however, determined by performing Gibbs ensemble simulations of the true binary colloidal rod-polymer mixture.[16] As there is no general expression for the effective polymer-mediated pair potential for two rods with arbitrary orientations and positions, Bolhuis *et al.* used a generalized square-well potential to draw some qualitative conclusions on the phase behavior of short-ranged attractive rods.[16] The crystal phase was, however, not included in this study.

In the present paper, we describe simulations of mixtures of colloidal hard rods and ideal polymer using the exact effective one-component Hamiltonian, i.e., it includes all the effective many-body interactions. We therefore extended our Monte Carlo simulation scheme[12,13] for the effective colloid Hamiltonian to rodlike particles. Employing this scheme, we are able to study the full phase diagram for arbitrary values of q. We compare our simulation results with those obtained from thermodynamic perturbation theory using the hard-spherocylinder system as reference state. In addition, we compare the phase diagrams with those obtained from simulations using the effective pair potential approximation to the effective Hamiltonian. This allows us to estimate the importance of the effective many-body interactions. We also propose a new two-parameter effective pair potential to approximate the volume of two overlapping depletion zones.

The paper is organized as follows. In Sec. II, we describe the model and present an explicit expression for the effective one-component Hamiltonian by integrating out the degrees of freedom of the polymer coils in the partition function. We also introduce the two-parameter effective pair potential to approximate the depletion pair potential, i.e., the volume of two overlapping depletion zones. In Sec. III we describe the simulation scheme based on the exact or full effective colloid Hamiltonian. In Sec. IV we present phase diagrams based on (i) the exact effective Hamiltonian, (ii) the exact effective Hamiltonian but using first-order perturbation theory, (iii) the effective pair potential approximation to the effective Hamiltonian, and (iv) an empiric effective depletion potential for the rods. We end with some concluding remarks.

II. MODEL

A. Effective Hamiltonian

A simple model for a mixture of sterically stabilized colloidal particles and nonadsorbing polymer is the so-called AO model.[3,4] In this model, the colloids are treated as hard particles, while the noninteracting polymer coils are treated as point particles, which are excluded from the surface of the colloids by a distance equal to the radius of gyration of the polymer R_g. The diameter of the polymer coils is $\sigma_p=2R_g$. The colloids are represented by hard spherocylinders, which consist of cylinders of diameter σ_c and length L with semispherical caps at both ends with diameter σ_c. The pair potentials in this model are given by

$$\phi_{cc}(\mathbf{R}_{ij};\hat{\omega}_i,\omega_j)=\begin{cases}\infty & \text{for } d_m(\mathbf{R}_{ij};\hat{\omega}_i,\hat{\omega}_j)<\sigma_c\\ 0 & \text{otherwise},\end{cases}$$

$$\phi_{cp}(\mathbf{R}_i-\mathbf{r}_j,\hat{\omega}_i)=\begin{cases}\infty & \text{for } d_m(\mathbf{R}_i-\mathbf{r}_j;\hat{\omega}_i)<\sigma_{cp}/2\\ 0 & \text{otherwise},\end{cases}$$

$$\phi_{pp}(r_{ij})=0,$$

where $\sigma_{cp}=\sigma_c+\sigma_p$, $\mathbf{R}_{ij}=\mathbf{R}_i-\mathbf{R}_j$ with $\mathbf{R}_i$ and $\mathbf{R}_j$ the center-of-masses of the spherocylinders and $d_m(\mathbf{R}_{ij};\hat{\omega}_i,\hat{\omega}_j)$ denotes the minimum distance between the central axes of the two spherocylinders with orientations $\hat{\omega}_i$ and $\hat{\omega}_j$, $d_m(\mathbf{R}_i-\mathbf{r}_j;\hat{\omega}_i)$ the minimum distance between the spherocylinder axis and the polymer center-of-mass at $\mathbf{r}_j$ in the case of colloid-polymer interactions, and $r_{ij}=|\mathbf{r}_i-\mathbf{r}_j|$ the distance between the two polymer center-of-masses.

The total Hamiltonian of a mixture of N_c colloidal rods and N_p ideal polymer coils in a volume V and at temperature T reads $H=H_{cc}+H_{cp}+H_{pp}$, where $H_{cc}=\Sigma_{i<j}^{N_c}\phi_{cc}(\mathbf{R}_{ij};\hat{\omega}_i,\hat{\omega}_j)$, $H_{cp}=\Sigma_{i=1}^{N_c}\Sigma_{j=1}^{N_p}\phi_{cp}(\mathbf{R}_i-\mathbf{r}_j;\hat{\omega}_i)$, and $H_{pp}=\Sigma_{i<j}^{N_p}\phi_{pp}(r_{ij})=0$.

In this paper, we map the rod-polymer mixture with interaction Hamiltonian H onto an effective one-component colloid system interacting with the effective Hamiltonian H^{eff}. Here we briefly sketch the derivation of a formal expression for the effective Hamiltonian for colloidal particles that possess orientational degrees of freedom, obtained by integrating out the degrees of freedom of the polymer coils in the partition function. For more details, we refer the reader to Refs. 9–13.

We fix the number of colloidal rods N_c and the fugacity $z_p=\Lambda_p^{-3}\exp(\beta\mu_p)$ of the polymer coils, where Λ_ν denotes the thermal wavelength of species $\nu=c,p$, μ_p the chemical potential of the reservoir of polymer coils, and $\beta=1/k_BT$ the inverse temperature. The thermodynamic potential $F(N_c,V,z_p,T)$ of this system can be written as

$$\exp[-\beta F]=\frac{1}{N_c!\Lambda_c^{3N_c}}\mathrm{Tr}_c\exp[-\beta H^{\text{eff}}], \tag{1}$$

where $H^{\text{eff}}=H_{cc}+\Omega$ and the trace Tr_c is short for the integrals over the coordinates and the orientations of the rods $\int_V d\mathbf{R}^{N_c}\int d\hat{\omega}^{N_c}$. Because of the ideal character of the polymer-polymer interactions in the AO model, $\beta\Omega$ simplifies to

$$-\beta\Omega=z_p\int_V d\mathbf{r}\exp\left[-\beta\sum_{i=1}^{N_c}\phi_{cp}(\mathbf{R}_i-\mathbf{r};\hat{\omega}_i)\right]=z_pV_f, \tag{2}$$

where $V_f=V_f(\{\mathbf{R};\hat{\omega}\};z_p)$ is the volume available for polymer, which depends on the static configuration of N_c colloidal rods with positions $\{\mathbf{R}_i\}$ and orientations $\{\hat{\omega}_i\}$; $i=1,2,\ldots,N_c$. Nonvanishing contributions to V_f stem from

those positions $\mathbf{r}$ that are outside any of the N_c depletion zones. Once V_f, and thus H^{eff}, are known for each colloidal rod configuration, the thermodynamics and the phase behavior of the mixture can be determined. We first show that V_f, and hence, the polymer-induced colloid interactions Ω can be split into zero-body, one-body, two-body, etc., contributions. To this end, we expand V_f in terms of the colloid-polymer Mayer function $f(\mathbf{R}_i-\mathbf{r};\hat{\omega}_i)$, which for the present model equals -1 for $0<d_m(\mathbf{R}_i-\mathbf{r};\hat{\omega}_i)<\sigma_{cp}/2$, and 0 otherwise, with $d_m(\mathbf{R}_i-\mathbf{r};\hat{\omega}_i)$ the minimum distance between the spherocylinder axis and position $\mathbf{r}$. We arrive at

$$V_f = \int d\mathbf{r} \prod_i^{N_c} [1+f(\mathbf{R}_i-\mathbf{r};\hat{\omega}_i)]$$
$$= V_f^{(0)} + \sum_i^{N_c} V_f^{(1)}(\mathbf{R}_i;\hat{\omega}_i) + \sum_{i<j}^{N_c} V_f^{(2)}(\mathbf{R}_i,\mathbf{R}_j;\hat{\omega}_i,\hat{\omega}_j) + \cdots$$
$$+ \sum_{i_1<\cdots<i_k}^{N_c} V_f^{(k)}(\mathbf{R}_{i_1},\ldots,\mathbf{R}_{i_k};\hat{\omega}_{i_1},\ldots,\hat{\omega}_{i_k}) + \cdots, \quad (3)$$

where the zero-body contribution $V_f^{(0)}$ is equal to the volume of the system V. For $k \geqslant 1$, we find

$$V_f^{(k)} = \int d\mathbf{r} \prod_{m=1}^{k} f(\mathbf{R}_{i_m}-\mathbf{r};\hat{\omega}_{i_m}). \quad (4)$$

The one-body contribution can be interpreted as the volume that is excluded for a polymer coil by a single rod. The two-body term is the overlap volume of two depletion zones of two colloidal rods. Introducing $n=n(\mathbf{r})\equiv-\sum_{i=1}^{N_c} f(\mathbf{R}_i-\mathbf{r};\hat{\omega}_i)$, the number of simultaneously overlapping depletion layers in $\mathbf{r}$, one finds the identity

$$\sum_{i_1<\cdots<i_k}^{N_c} V_f^{(k)}(\mathbf{R}_{i_1},\ldots,\mathbf{R}_{i_k}) = (-1)^k \int_{n\geqslant k} d\mathbf{r} \frac{n(\mathbf{r})!}{(n(\mathbf{r})-k)!k!}. \quad (5)$$

All $k' \geqslant k$ terms in Eq. (3) can be summed to obtain (for the present Mayer function only)

$$V_f^{(k+)} = \sum_{k'\geqslant k} \left[\sum_{i_1<\cdots<i_{k'}}^{N_c} V_f^{(k')}(\mathbf{R}_{i_1},\ldots,\mathbf{R}_{i_{k'}};\hat{\omega}_{i_1},\ldots,\hat{\omega}_{i_{k'}}) \right]$$
$$= \frac{(-)^k}{(k-1)!} \int_{n\geqslant k} d\mathbf{r} \prod_{i=1}^{k-1} (n(\mathbf{r})-i). \quad (6)$$

The terms $V_f^{(0)}, V_f^{(1)}$ are irrelevant offsets that do not influence the thermodynamic properties of the bulk mixture.[11] Setting $V_f^{(3+)}$ equal to zero, the pairwise additivity approximation is recovered.

B. Effective pair potential description

In the case of spherical colloids, it can be shown explicitly that for sufficiently small polymer coils, the three-body and higher-body terms are identially zero, and that the mapping onto an effective Hamiltonian truncated at the effective pair potential level is exact. Hence, the pairwise additivity approximation to the effective Hamiltonian, i.e., $V_f^{(3+)}=0$, proves to be a reasonable approximation to predict the phase behavior of the AO model for polymer coils that are small compared to the size of the colloids. For spherical colloids, the effective pair potential is given by the Asakura-Oosawa depletion potential,[3] which is known analytically, while $V_f^{(3+)}$ can only be evaluated numerically.[13] In the case of colloidal rods, the overlap volume of two infinitely long cylindrical depletion zones can be calculated exactly.[17,18] However, no analytic expression exists for the overlap volume of two depletion zones of finite spherocylinders with arbitrary orientations and positions and, hence, $V_f^{(2)}$ can only be calculated numerically. The numerical evaluation of $V_f^{(2)}$ is almost as expensive as $V_f^{(2+)}$ that includes all the effective many-body interactions. It is therefore useful to have a good model pair potential that is mathematically simple and fits reasonably well the exact overlap volume of two depletion zones. Bolhuis *et al.*[16] approached this problem by using a generalized square-well potential, which provides qualitatively correct phase diagrams, when the size of the polymer is small compared to the diameter of the rods. It lacks, however, quantitative agreement with the exact overlap volume of the depletion zones of two spherocylinders, thereby overestimating significantly the attraction (especially at larger distances).

Here we propose a two-parameter pairwise additive depletion potential $\beta\phi_{\text{dep}}(\mathbf{R}_{ij},\hat{\omega}_i,\hat{\omega}_j)$ to approximate the exact overlap volume of the depletion zones of two spherocylinders $V_{\text{overlap}}(\mathbf{R}_{ij},\hat{\omega}_i,\hat{\omega}_j)$, and hence $\beta\phi_{\text{dep}}(\mathbf{R}_{ij},\hat{\omega}_i,\hat{\omega}_j) \simeq -z_p V_f^{(2)} = -z_p V_{\text{overlap}}(\mathbf{R}_{ij},\hat{\omega}_i,\hat{\omega}_j)$. We start with the assumption that the overlap volume of the depletion zones can be fitted by the overlap of two axially symmetric anisotropic Gaussian functions. The overlap integral of two Gaussian distributions can be calculated exactly to give[19]

$$\phi_{\text{dep}}(\mathbf{R}_{ij},\hat{\omega}_i,\hat{\omega}_j) = \varepsilon(\hat{\omega}_i,\hat{\omega}_j) e^{-R_{ij}^2/\sigma(\hat{\mathbf{R}}_{ij},\hat{\omega}_i,\hat{\omega}_j)^2}, \quad (7)$$

where $\hat{\mathbf{R}}_{ij}$ is the unit vector in the direction of the center-of-mass distance of two rods, $R_{ij}\equiv|\mathbf{R}_i-\mathbf{R}_j|$, $\varepsilon(\hat{\omega}_i,\hat{\omega}_j)$ is the angle-dependent strength parameter given by $\varepsilon(\hat{\omega}_i,\hat{\omega}_j) = \varepsilon_0(1-\chi^2(\hat{\omega}_i\cdot\hat{\omega}_j)^2)^{-1/2}$, with the parameter χ determined by the anisotropy of the particles, and $\sigma(\hat{\mathbf{R}}_{ij},\hat{\omega}_i,\hat{\omega}_j)$ is the angle-dependent range parameter. Various modifications of these single site potentials with angle-dependent strength and range parameters exist[20–22] tailored to fit the wide range of anisotropic interactions.

Here we construct a modified single site potential that fits reasonably well the exact overlap volume of the depletion zones. The first modification is to replace the center-to-center distance R_{ij} in (7) to the minimum distance $x = d_m(\mathbf{R}_{ij};\hat{\omega}_i,\hat{\omega}_j)/\sigma_{cp}$ between the spherocylinder axes together with a replacement of the angle-dependent range parameter $\sigma(\hat{\mathbf{R}}_{ij};\hat{\omega}_i,\hat{\omega}_j)$ by simply the isotropic interaction range σ_{cp}, such that the range of the potential at the minimum distance is independent of the orientation. The second modification is to replace the Gaussian potential in Eq. (7) by a more realistic expression. The first option is to use the volume excluded by two spheres, which fits accurately the interaction of perpendicular cylinders, or parallel ellipsoids. Moreover this choice is convenient for an extrapolation from hard rods to hard spheres using a Parsons approach. As this

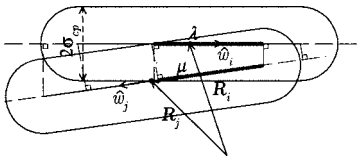

FIG. 1. A schematic sketch of the interaction lengths for two spherocylinders with a length-to-diameter ratio L/σ_c and nonadsorbing polymer coils with diameter σ_p. The positions and the orientations of the spherocylinders are denoted by $\mathbf{R}_i$, $\mathbf{R}_j$, $\hat{\omega}_i$, and $\hat{\omega}_j$. The interaction length is defined as the length of that part of the cylinder axis of the spherocylinder for which there are points on the axis of the other spherocylinder within a distance σ_{cp}. Moreover, the interaction length should also satisfy a second constraint, which can be determined as follows. Take the shortest distance from the two end points of one spherocylinder axis to the other spherocylinder axis. This yields two points on the central axis of the other spherocylinder (or an extension thereof). The interaction length should lie in between these two points. The interaction lengths μ and λ are denoted by the thick lines.

paper is focused on the liquid crystalline behavior of elongated rods, we use here the overlap volume of two parallel cylinders with diameter σ_{cp} per unit length at a minimum distance x,

$$f(x) = \frac{\sigma_{cp}^2}{2}[\arccos(x) - x\sqrt{1-x^2}]. \tag{8}$$

In addition, we define a new strength parameter, which is a function of $\hat{\omega}_i$ and $\hat{\omega}_j$ as well as on $\mathbf{R}_{ij}$. To this end, we replace the anisotropy parameter χ in $\varepsilon(\mathbf{R}_{ij};\hat{\omega}_i,\hat{\omega}_j)$ by an angle- and distance-dependent anisotropy parameter $\chi(\mathbf{R}_{ij};\hat{\omega}_i,\hat{\omega}_j)$, which is used to ensure that the overlap volume remains constant when two nonparallel cylinders slide along each other, and changes when two nearly parallel rods shift along each other. To achieve this, we introduce the concept of interaction length, which can be interpreted as the length of the spherocylinder that is felt by the other spherocylinder. We illustrate this in Fig. 1. This length is defined as the length of that part of the central axis of the spherocylinder for which there are points on the axis of the other spherocylinder within a distance σ_{cp}, i.e., that part of the cylinder that lies within the other spherocylinder with a length-to-diameter ratio $L/2\sigma_{cp}$. The anisotropy parameter is now based not on the actual length and diameter of the spherocylinder, but rather on the interaction length of the two spherocylinders, say, λ and μ. For large polymer diameters, however, it is possible that when two aligned spherocylinders shift along each other, they still feel each other by the full length of the cylinder axis even for considerable shifts. We correct this by the following constraint. We take the shortest distance from the two end points of one spherocylinder axis to the other spherocylinder axis. This yields two points on the central axis of the other spherocylinder (or an extension thereof). Our second constraint is that the interaction length lies between these two points.

The anisotropy parameter for two identical ellipsoids was calculated by Berne and Pechukas.[19] Here, we use a simple multiplication of the square root of the anisotropy parameter of an ellipsoid with major and minor axes $\lambda+\sigma_{cp}$ and σ_{cp} times the square root of the anisotropy parameter of an ellipsoid with major and minor axes $\mu+\sigma_{cp}$ and σ_{cp}.

$$\chi(\mathbf{R}_{ij};\hat{\omega}_i,\hat{\omega}_j) = \chi^2(\lambda,\mu) = \frac{(\xi\lambda+\sigma_{cp})^2-(\sigma_{cp})^2}{(\xi\lambda+\sigma_{cp})^2+(\sigma_{cp})^2}\frac{(\xi\mu+\sigma_{cp})^2-(\sigma_{cp})^2}{(\xi\mu+\sigma_{cp})^2+(\sigma_{cp})^2}. \tag{9}$$

Moreover, we introduce the fitting parameter ξ to correct for the difference in overlap volumes of ellipsoids and of spherocylinders. This anisotropy parameter yields the correct results for identical rods and vanishes in the case when only the spherocylinder cap interacts with the cylinder, i.e., when μ or λ equals zero.

Finally, our modified two-parameter depletion pair potential that approximates the exact overlap volume of two depletion zones reads

$$\phi_{\text{dep}}(\mathbf{R}_{ij},\hat{\omega}_i,\hat{\omega}_j) = \frac{\varepsilon_0\sigma_{cp}^2}{2}\frac{\arccos(x)-x\sqrt{1-x^2}}{\sqrt{1-\chi^2(\lambda,\mu)(\hat{\omega}_i\cdot\hat{\omega}_j)^2}}, \tag{10}$$

with $\chi^2(\lambda,\mu)$ given by (9). The two fitting parameters ε_0 and ξ can be determined independently from each other. To this end, we employed a fit of $\int drr\exp(z_pV_{\text{overlap}}) = \int drr\exp(-\beta\phi_{\text{dep}})$ for a pair of spherocylinders that are perpendicular to each other and for two spherocylinders that are parallel. The exact overlap volume of two depletion zones V_{overlap} can be calculated analytically in a few cases or otherwise numerically. We like to stress that for spherocylinders of fixed diameter σ_c and polymer size σ_p, ξ is rather independent of the spherocylinder length L, which justifies the use of the interaction length. Figure 2 shows the good agreement between the exact overlap volume with the two-parameter depletion pair potential (10) for a system of colloidal hard rods with $L/\sigma_c=5$ and nonadsorbing polymer coils with diameter σ_p and $q=\sigma_p/\sigma_c=0.5$. The values of the fitting parameters are displayed in Table I for the size ratios employed in this work.

III. SIMULATIONS

In Sec. II we derived the effective Hamiltonian of the colloids by integrating out the degrees of freedom of the polymer coils in the partition function. The key quantity in the effective Hamiltonian is the available volume V_f for the polymer coils which depends on the instantaneous colloid positions $\{\mathbf{R}_i\}$ and orientations $\{\hat{\omega}_i\}$. We calculate V_f numerically on a smart grid, which allows us to employ the full effective Hamiltonian or to employ the pairwise additivity assumption for the effective Hamiltonian by setting $V_f^{(3+)}=0$. As already noted in Refs. 12 and 13, the standard Metropolis algorithm in Monte Carlo simulations is based on the acceptance probability $\min(1,\exp[-\beta\Delta H^{\text{eff}}])$, with ΔH^{eff} the change of H^{eff} due to a displacement of a single colloidal rod at position $\mathbf{R}_1\rightarrow\mathbf{R}_1'$ with orientation $\hat{\omega}_1\rightarrow\hat{\omega}_1'$. The only contributions to ΔV_f and hence to ΔH^{eff} occurs inside the two spherocylinders with length-to-diameter ratio L/σ_{cp} centered about $\mathbf{R}_1$ with orientation $\hat{\omega}_1$ and about $\mathbf{R}_1'$ with orientation $\hat{\omega}_1'$. We mesh these two spherocylinders by a uniform grid with typically $(0.8-1.8)\times10^6$ grid points. It is convenient to use the coordinate frame of the spherocylinder, in which the central axis of the spherocylinder coincides with the z axis.

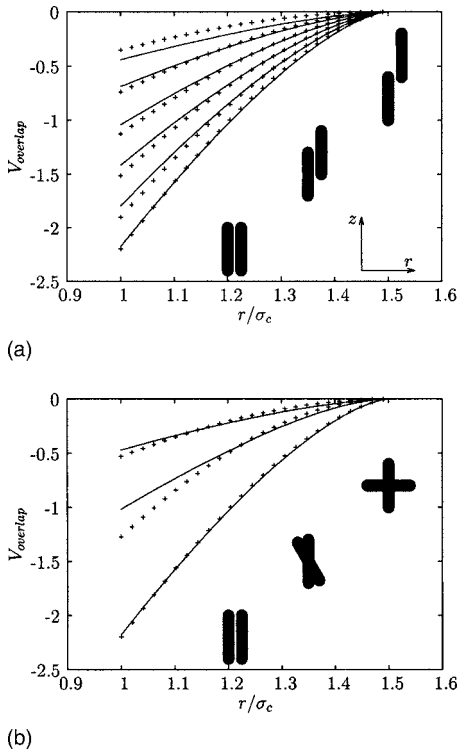

FIG. 2. The negative of the exact overlap volume of two depletion zones $-V_{\text{overlap}}$ (plusses) and the approximate effective pair potential (solid lines) for two spherocylinders with $L/\sigma_c=5$, and $\sigma_p/\sigma_c=0.5$ as a function of a center-of-mass displacement in the r direction. (a) Parallel spherocylinders oriented in the z direction for a fixed shift of the center of mass of the second spherocylinder in the z direction. The curves from bottom to top denote a shift of $z/\sigma_c=0,1,2,3,4,5$. (b) Two spherocylinders with zero z shift, the second one rotated about the line through the center of masses by $\theta=0$, arccos(12/13), $\pi/2$ from bottom to top.

Subsequently, all the other spherocylinders, whose depletion zones overlap with the depletion zone of this spherocylinder, are transformed to this coordinate frame. We also correct for the grid points that belong to both grids of the spherocylinders.

We performed *NVT* Monte Carlo simulations of the isotropic and nematic phase using 762 particles in a cubic box. For the smectic and crystal phases, we employed 462 and 240 particles, respectively. In addition, we allowed for box shape fluctuations during our simulations of the smectic and crystal phases, while the total volume of the system was kept fixed. Equilibration is checked by monitoring the free volume accessible for the polymers. In order to determine the phase diagram of the effective one-component system, we first calculate the thermodynamic potential F, defined in Eq. (1), as a function of N_c, V, z_p. The polymer fugacity z_p is related to the reservoir packing fraction $\eta_p^r \equiv \pi\sigma_p^3 z_p/6$. We use thermodynamic integration to relate the free energy $F(\eta_c, z_p)$ of the effective system to that of a reference system of pure hard rods at the same colloidal rod packing fraction $\eta_c \equiv \pi\sigma_c^3(1+3/2L\sigma_c)N_c/6V$.

TABLE I. The values of the fitting parameters ε_0 and ξ of the two-parameter depletion potential for a system of colloidal hard rods with a length-to-diameter ratio $L/\sigma_c=5$ and nonadsorbing polymer coils with diameter σ_p and varying diameter ratios $q=\sigma_p/\sigma_c$.

q	$\varepsilon_0/2$	ξ
0.15	0.277 089	4.144 77
0.50	0.546 528	2.747 85
1.00	0.875 059	2.293 93

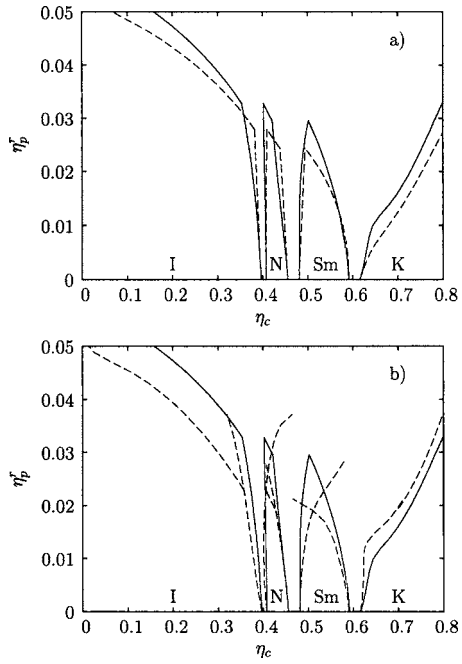

FIG. 3. Phase diagrams for a mixture of hard spherocylinders with $L/\sigma_c=5$ and nonadsorbing polymer coils with a diameter σ_p. The size ratio $q=\sigma_p/\sigma_c=0.15$. (a) Phase diagram based on the full effective Hamiltonian, i.e., including all effective many-body interactions, thermodynamic integration (—), first-order perturbation theory (- - -), and (b) phase diagram based on the effective pair potential approximation to the effective Hamiltonian, i.e., $V_f^{(3+)}=0$ (—), and using the two-parameter effective depletion potential (10) (--).

$$\beta F(\eta_c, z_p) = \beta F(\eta_c, 0) - \int_0^{z_p} dz_p' \langle V_f(z_p') \rangle. \tag{11}$$

The free energies for the reference system of pure hard spherocylinders are determined from the equation-of-state data obtained from simulations of Ref. 23. The thermodynamic integration is based on typically 20–30 points in the (η_c, z_p) plane for each phase. Once the free energies are known for each phase as a function of η_c and z_p, we can determine the densities of the coexisting phases by equating the pressures and chemical potentials in both phases.

IV. RESULTS AND DISCUSSION

The procedure described above was used to determine the phase behavior of mixtures consisting of colloidal hard rods with a length-to-diameter ratio $L/\sigma_c=5$ and nonadsorbing polymer coils with a radius of gyration $R_g=\sigma_p/2$. We mapped out the phase diagram for diameter ratios $q=\sigma_p/\sigma_c=0.15$, 0.5, and 1. Fig. 3 shows the phase diagrams for $q=0.15$ in the (η_c, η_p^r) plane. In Fig. 3(a), we present the resulting phase diagram based on the full effective many-body Hamiltonian. The binodals are shown by the solid lines. In this representation, the tie lines connecting coexisting state points are horizontal. The phase diagrams show thermody-

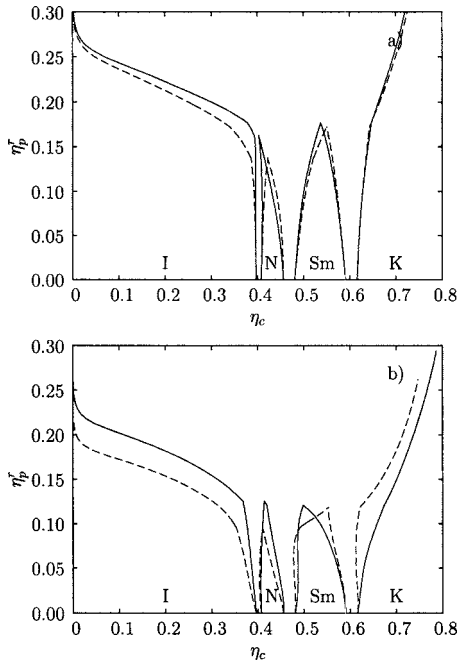

FIG. 4. Same as in Fig. 3, but for $q=0.5$.

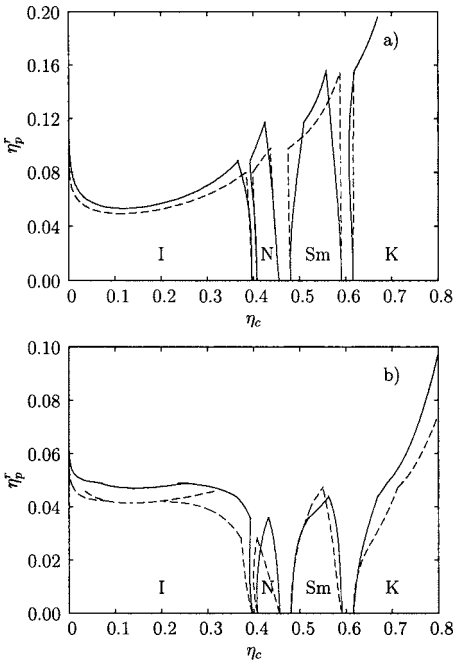

FIG. 5. Same as in Fig. 3, but for $q=1$.

namically stable regions of the isotropic (I), nematic (N), smectic-A (Sm), and crystalline (K) phases. At $\eta_p^r=0$, we recover the I-N, N-Sm, Sm-K transition of the pure hard-rod system. Increasing η_p^r, we observe an enormous broadening of the Sm-K coexistence region, while the I-N and N-Sm coexistence region broadens only slightly. We also find that the smectic phase becomes metastable with respect to the nematic phase for η_p^r higher than the N-Sm-K triple point, resulting in a broad N-K coexistence region. At slightly higher η_p^r, the phase diagram shows an I-N-K triple point and an I-K coexistence, which widens upon increasing η_p^r. For comparison, we also plot the phase diagram based on first-order perturbation theory (dashed lines), where we assume that the available free volume for the polymer does not depend on the polymer fugacity, i.e., we set $V_f(\eta_c,z_p)=V_f(\eta_c,0)$. We observe that in first-order perturbation theory all the binodals and triple points are slightly shifted to lower polymer reservoir packing fractions compared to the exact phase diagrams. For this size ratio the mapping of the binary mixture onto an effective one-component system with only effective pair potentials, i.e., $V_f^{(3+)}=0$, is exact. In Fig. 3(b), we compare the phase diagram based on the effective pair potential description to the effective Hamiltonian (solid lines) with the one based on the two-parameter effective depletion potential (10) (dashed lines). Figure 3(b) shows that employing the effective depletion potential yields a shift of the binodals to lower polymer reservoir packing fractions, but the overall agreement is reasonable.

In Fig. 4, we present the phase diagrams for $q=0.5$. We now observe a broadening of both the N-Sm and the Sm-K coexistence region upon increasing η_p^r. At sufficiently high η_p^r, an I-N-Sm triple point and subsequently, a broad I-Sm coexistence region appears. At slightly higher η_p^r, we find a I-Sm-K triple point and a broad I-K coexistence region, which widens even further upon increasing η_p^r. The first-order perturbation theory (dashed lines) results again in a shift of all binodals towards lower polymer reservoir packing fractions. For $q=0.5$, the effective three- and higher-body many-body interactions are not identical to zero, and Fig. 4(b) shows the phase diagram based on the effective pair potential approximation to the effective Hamiltonian (solid lines), i.e., $V_f^{(3+)}=0$. We find that neglecting the effective many-body interactions results in a shift of the broad I-K coexistence region to lower η_p^r, and it widens the I-N coexistence region. Figure 4(b) also shows the phase diagram based on the two-parameter effective depletion potential (10) (dashed lines). Again, we find that employing the effective depletion potentials results in a shift of the binodals to lower polymer reservoir packing fractions.

In Fig. 5, we present the phase diagrams for $q=1$. We now observe a slight widening of the N-Sm and the Sm-K coexistence region upon increasing η_p^r. Moreover, we find at sufficiently high η_p^r, an I-I coexistence region ending in a critical point. For polymer packing fraction higher than the critical point a phase separation occurs in an isotropic "gas" phase which is dilute in colloidal rods and an isotropic "liquid" phase which is dense in rods. Upon increasing η_p^r, an I-I-N triple point is found and the liquid phase becomes metastable with respect to the nematic phase. A broad I-N coexistence region is observed for η_p^r higher than the I-I-N triple point. Upon increasing η_p^r, we observe successively an I-N-Sm triple point, a broad I-Sm coexistence, an I-Sm-K triple point, and finally, a broad I-K coexistence region. First-order perturbation theory (dashed lines) shows an overall shift of all binodals, triple points, and the critical point towards lower polymer reservoir packing fractions. Figure 4(b) shows the phase diagram based on the effective pair potential approximation to the effective Hamiltonian (solid line). We find that the main effect of the many-body interactions is that the I-I demixing transition is enhanced and that the binodals

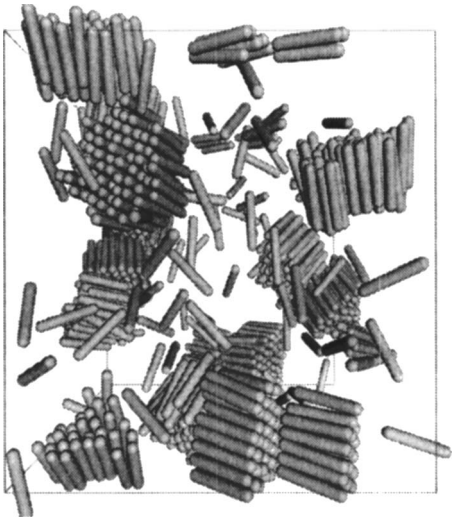

FIG. 6. Typical configuration of a mixture of colloidal hard rods with $L/\sigma_c=5$ and nonadsorbing polymer (not visible) with $q=0.5$ well inside the broad isotropic-crystal coexistence region at a colloidal rod packing fraction $\eta_c=0.0884$ and a polymer reservoir packing fraction $\eta_p^r=0.26$ using the semi-empiric potential (10).

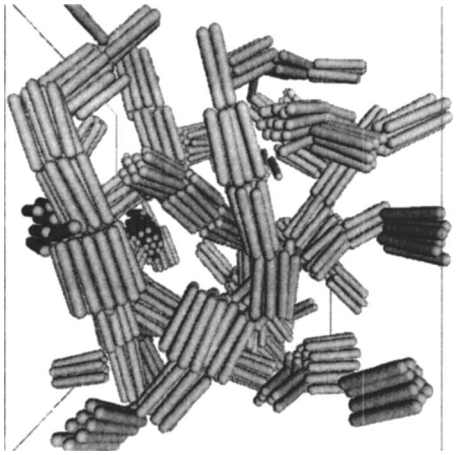

FIG. 7. Same as Fig. 6, but at $\eta_p^r=0.32$.

are shifted to higher η_p^r. Moreover, we find that the nematic and smectic phases are stabilized by the many-body interactions, resulting in broad *I*-*N* and *I*-Sm coexistence regions. Figure 4(b) also shows the phase diagram based on the two-parameter effective depletion potential (10) (dashed lines). Again, we find that employing the effective depletion potential results in a shift of the binodals to lower polymer reservoir packing fractions.

In summary, we find that the phase diagram for large polymer coils displays an isotropic "gas-liquid" phase separation ending in a critical point and an *I*-*I*-*N* triple point. Moreover, the phase diagram shows *I*-*N*-Sm and *I*-Sm-*K* triple points and broad coexistence of *I*-*N*, *I*-Sm, and *I*-*K* phases. For smaller polymer coils, we find that the polymer reservoir packing fractions of the *I*-*N*-Sm triple point moves to higher values and consequently, we only find broad *I*-*K* coexistence regions. Reducing the polymer coils even further, we observe an *I*-*N*-*K* and a *N*-Sm-*K* triple point. The topologies of these phase diagrams as a function of q are consistent with the first-order perturbation theory calculations in Ref. 16. In addition, we find that the two-parameter depletion potential yields reasonable agreement with the exact phase diagrams, in particular, at small q. This potential can be used in nucleation studies where the simulations based on the exact effective Hamiltonian is computationally too expensive. Very recent experiments on mixtures of fd virus particles and dextran (nonadsorbing polymer) by Dogic and Fraden showed different kinetic pathways of the formation of the smectic or crystal phase as a function of the exact dextran concentration.[24] At low polymer concentrations, they observe the nucleation of colloidal membranes that consist of a single layer of rods, which can coalesce laterally. At higher polymer concentrations, the membranes can stack on top of each other to form long thin filaments. Figures 6 and 7 show typical configurations of a mixture of colloidal hard rods with $L/\sigma_c=5$ and nonadsorbing polymer (not visible) with a diameter ratio $q=0.5$ well inside the broad isotropic-crystal coexistence region at $\eta_c=0.0884$, $\eta_p^r=0.26$ and at $\eta_c=0.0884$, $\eta_p^r=0.32$, respectively, using the semi-empiric potential (10). In Fig. 6, we find the formation of single membranes, while Fig. 7 shows the formation of long filaments. These results are in agreement with these experimental findings. Note that we ignored completely in our "integrating out procedure" the possibility of gel formation at very high polymer concentrations. In order to take this into account, one should resort to more detailed and expensive simulations of the true binary mixture that includes a realistic description of the polymers. The formation of filaments was studied theoretically by Frenkel and Schilling.[25] The nucleation of the crystal phase in a pure fluid of hard rods ($\eta_p^r=0$) with $L/\sigma_c=2$ was investigated in an earlier simulation study.[26] This work shows that in the earliest stages of nucleation, a colloidal crystalline membrane is formed, but nucleation growth is then hampered by the fact that the top and bottom surfaces of this crystallite are preferentially covered by rods that align parallel to the surface; the surface poisons itself.[26] For the length-to-diameter ratio considered in this work, i.e., $L/\sigma_c=5$, we find a sequence of *I*-*N*, *N*-Sm, and Sm-*K* transitions upon increasing the density at $\eta_p^r=0$, in contrast with a direct transition from the isotropic fluid to the crystalline phase for $L/\sigma_c=2$. Preliminary nucleation studies of a pure fluid of hard rods with $L/\sigma_c=5$ show the nucleation and growth of the nematic phase in a supersaturated isotropic phase without any self-poisoning.[27] As the nematic (smectic) phase is orientationally ordered, we do not expect self-poisoning in the case of the smectic (crystal) nucleation for $L/\sigma_c=5$. More detailed nucleation studies of mixtures of colloidal rods with polymer-mediated effective attractions will be the future work.

[1] S. S. Cohen, J. Biol. Chem. **144**, 353 (1942).
[2] P. Buining, Y. S. J. Veldhuizen, C. Pathmamamnoharan, and H. N. W. Lekkerkerker, Colloids Surf. **64**, 47 (1992).
[3] S. Asakura and F. Oosawa, J. Chem. Phys. **22**, 1255 (1954).
[4] A. Vrij, Pure Appl. Chem. **48**, 471 (1976).
[5] A. P. Gast, C. K. Hall, and W. B. Russel, J. Colloid Interface Sci. **96**, 251 (1983).
[6] H. N. W. Lekkerkerker, W. C. K. Poon, P. N. Pusey, A. Stroobants, and P. B. Warren, Europhys. Lett. **20**, 559 (1992).
[7] E. J. Meijer and D. Frenkel, Phys. Rev. Lett. **67**, 1110 (1991).
[8] E. J. Meijer and D. Frenkel, J. Chem. Phys. **100**, 6873 (1994).

[9] M. Dijkstra, R. van Roij, and R. Evans, Phys. Rev. Lett. **81**, 2268 (1998).
[10] M. Dijkstra, R. van Roij, and R. Evans, Phys. Rev. Lett. **82**, 117 (1999).
[11] M. Dijkstra, R. van Roij, and R. Evans, Phys. Rev. E **59**, 5744 (1999).
[12] M. Dijkstra and R. van Roij, Phys. Rev. Lett. **89**, 208303 (2002).
[13] M. Dijkstra, R. van Roij, R. Roth, and A. Fortini, Phys. Rev. E **73**, 041404 (2006).
[14] M. Dijkstra, Curr. Opin. Colloid Interface Sci. **6**, 372 (2001).
[15] M. Dijkstra, J. M. Brader, and R. Evans, J. Phys.: Condens. Matter **11**, 10079 (1999).
[16] P. G. Bolhuis, A. Stroobants, D. Frenkel, and H. N. W. Lekkerkerker, J. Chem. Phys. **107**, 1551 (1997).
[17] P. B. Warren, J. Phys. (France) **4**, 237 (1994).
[18] C. W. Trigg, *Mathematical Quickies* (Dover, New York, 1985).
[19] B. J. Berne and P. Pechukas, J. Chem. Phys. **56**, 4213 (1972).
[20] S. H. Walmsley, Chem. Phys. Lett. **49**, 390 (1977).
[21] J. G. Gay and B. J. Berne, J. Chem. Phys. **74**, 3316 (1981).
[22] B. Martinez-Haya, A. Cuetos, S. Lago, and L. F. Rull, J. Chem. Phys. **122**, 024908 (2005).
[23] P. Bolhuis and D. Frenkel, J. Chem. Phys. **106**, 666 (1997).
[24] Z. Dogic and S. Fraden, Philos. Trans. R. Soc. London, Ser. A **359**, 997 (2001).
[25] D. Frenkel and T. Schilling, Phys. Rev. E **66**, 041606 (2002).
[26] T. Schilling and D. Frenkel, Phys. Rev. Lett. **92**, 085505 (2004).
[27] A. Cuetos and M. Dijkstra (unpublished).